

Article

Corrosion Mechanism of A Density-Reduced Steel Ladle Lining Containing Porous Spinel-Calcium Aluminate Aggregates

Christoph Wöhrmeyer ^{1,*}, Jianying Gao ¹, Christopher Parr ¹, Magali Szepezdyn ¹,
Rose-Marie Mineau ¹ and Junhui Zhu ²

¹ Imerys S.A., 75015 Paris, France; simon.gao@imerys.com (J.G.); chris.parr@imerys.com (C.P.); magali.szepezdyn@imerys.com (M.S.); rose-marie.mineau@imerys.com (R.-M.M.)

² Jinan New E'mei Co., Ltd., Jinan 0531, China; 13864083529@163.com

* Correspondence: christoph.wohrmeyer@imerys.com

Received: 2 December 2019; Accepted: 18 March 2020; Published: 23 March 2020



Abstract: Refractory monolithics for steel ladle linings are typically products with low porosities and high bulk densities. They achieve high temperature, penetration, and corrosion resistance. Despite the high density of these products, which is due to the low porosity of the aggregates, their matrices still exhibit a high amount of pores. Since calcium magnesium aluminate (CMA) has already proven its resistance to penetration and corrosion as a binder in the matrix, this paper investigated if alumina spinel refractories containing microporous calcium magnesium aluminate aggregates can withstand conditions that occur in a steel ladle wall. The objective was to reduce the castable density with the advantage of a lower material requirement for a ladle lining and reduced heat and energy losses. This was achieved by replacing dense alumina aggregates by up to 38% of porous CMA aggregates (grains with 30 vol% porosity), which resulted in a bulk density reduction from 3.1 g/cm³ for the dense alumina castable to 2.8 g/cm³ for the 38% CMA aggregates containing castable. However, the despite the higher porosity, penetration, and corrosion resistance and thermomechanical properties were not impacted negatively for a model alumina spinel castable. A postmortem investigation was conducted on a newly developed dry-gunning mix that was installed in a steel ladle wall on top of a slag penetrated castable and that achieved a service life of 31 heats versus only 18 heats for the reference mix that contained dense alumina and spinel aggregates. This new repair mix contained the newly designed porous CMA aggregates, which in this case partly replaced the dense alumina and spinel aggregates. These porous aggregates consisted of magnesium aluminate and calcium aluminate micro-crystals. The postmortem study revealed two important phenomena that can explain the improved performance: at the hot face in contact with steel and slag, a thin densified zone was observed that blocked the slag penetration into the porous matrix and the porous aggregates. Iron oxides were almost completely blocked from penetration, and only some manganese oxide was observed in the penetrated zone together with some silica and lime from the slag. Clusters of calcium aluminate (CA₆) and magnesium aluminate (MA) spinel build the refractory back-bone on the hot side of the material and gussets filled with mostly glassy calcium aluminum silicates close to the hot face and gehlenite further inside the penetrated zone. Alumina grains had a reaction rim consisting of CA₂ or CA₆ and a very intimate connection to the surrounding matrix unlike the CMA-free mix that showed micro cracks around the alumina grains. At the colder side, the gunning mix with CMA aggregates showed a very good connection to the substrate, supported by a hercynite formation in the gunning mix resulting from a cross-reaction with remains of iron oxide on the CMA containing repair mix. Furthermore, macroscopic observations of a CMA aggregate containing alumina magnesia castable in the metal zone of a steel ladle revealed that macro cracks developed only very slowly, which resulted in a superior service life.

Keywords: steel ladle; refractory; corrosion; spinel; calcium aluminate; density; porosity

1. Introduction

Steel ladle linings with spinel-containing or spinel-forming high alumina refractories in the metal zone (wall and bottom) are the state-of-the-art [1–3]. While magnesia-carbon refractories potentially pollute steel with carbon [4], the high purity and carbon-free alumina spinel refractories facilitate the production of ultra-low carbon steel. Traditionally, ladle castable developers try to minimize slag penetration by selecting aggregates with as low as possible porosity and by obtaining a low porosity matrix using an optimized particle size distribution by employing micro powders dispersed with highly efficient additives. In the case of castables, the latest generation poly-carboxylate ether additives enable high fluidity at the lowest possible amount of mixing water. The bulk densities of dried alumina spinel and alumina magnesia refractories are typically close to 3 g/cm³ [5,6]. Nevertheless, the porosity of the matrix remains still significantly higher than the porosity of the aggregates and represents the weakest part of the refractory material with respect to slag penetration and corrosion. However, studies have shown that matrix compositions with a homogeneous distribution of micro-crystalline magnesium aluminate spinel (MA spinel), calcium mono-aluminate (CA), calcium di-aluminate (CA₂), and alumina (A) can counteract the penetration and corrosion [7]. In the matrix, an improved resistance against penetration and corrosion was observed when using a calcium magnesium aluminate binder (CMA72, Imerys, Paris) [7,8].

Previous studies by Yan et al. [9] demonstrated that while keeping the matrix composition constant, a significant increase of the apparent porosity of alumina aggregates from 4% to 24% and even 42% resulted in a significant increase of penetration and corrosion. Fu et al. [10] compared tabular alumina with an apparent porosity of 2.8% (closed porosity 5%) with a microporous corundum that had 4.1% apparent porosity (10.1% closed porosity). They measured a reduction of thermal conductivity and found surprisingly a somewhat improved corrosion resistance of alumina magnesia castable when using those microporous aggregates. Chen et al. [6] found that a low density castable for a steel ladle can be developed by using low density MA spinel aggregates. Decreasing the density of the aggregates did not negatively impact the durability of the castable. Application of the low density castable resulted in a decrease of the material consumption and thermal conductivity of the ladle lining. Furthermore, alumina castables with additions of 10–35% MA spinel have proven to be more penetration and corrosion resistant than pure alumina castables [11].

This paper brings two separate earlier studies [12,13] into a broader context and investigates if the specific matrix phase assemblage of alumina spinel castable, consisting of MA, CA, CA₂, and A (prior to firing), could also have a benefit when applied as porous aggregates consisting of micro-crystalline MA, CA, and CA₂. Such MA-CA-CA₂ aggregates have been developed (MagArmour (MagA), Imerys, France) and successfully used as additive to magnesia-carbon (MgO-C) bricks for steel ladle linings [14]. In MgO-C bricks, they contribute to an in situ formation of a protective slag layer on the surface of the bricks. If those porous MagA aggregates could be used in alumina spinel refractories and keep sufficient resistance against slag penetration and corrosion, the benefits could be:

- a lower material requirement per ladle lining;
- a lower energy loss through the refractory lining;
- an improved thermal shock resistance.

Laboratory trials with model alumina spinel ladle castables have been conducted to investigate the rheological and thermo-physical aspects of lightening ladle castables with the porous MagA aggregate. Static corrosion trials with ladle slag have been conducted to compare the penetration and corrosion resistance with a reference alumina spinel castable that only contains dense aggregates (alumina and spinel). Industrial trials with a commercial alumina spinel dry-gunning mix have been conducted.

Postmortem samples from this industrial trial served as the basis for the investigation of the penetration and corrosion mechanism of the lightened alumina spinel castable.

2. Materials and Methods

Four different MagA aggregate fractions (0–1 mm, 1–3 mm, 3–5 mm, 5–10 mm) were prepared by crushing and sieving a sintered clinker containing in each grain a micro-phase assemblage consisting of MA spinel, CA_2 , and CA. They consisted of about 70% microcrystalline magnesium aluminate spinel and 30% calcium aluminates. The detailed chemistry and mineralogy of MagA are shown in Table 1. Figure 1 shows the porous microstructure of MagA. The apparent grain porosity was close to 30 vol%, while it was significantly less than 10 vol% for the reference aggregates, tabular alumina (TA), white fused alumina (WFA), and magnesium aluminate spinel (MA spinel). For MagA, a pyrometric cone equivalent (PCE) of over 1700 °C was measured, sufficiently high to formulate alumina spinel castables for steel ladle applications.

Table 1. Composition of MagArmour (MagA) aggregate.

Chemistry	Al_2O_3	MgO	CaO
wt%	70.5	20.5	9
Mineralogy	MA spinel	CA	CA_2
wt%	70	20	10

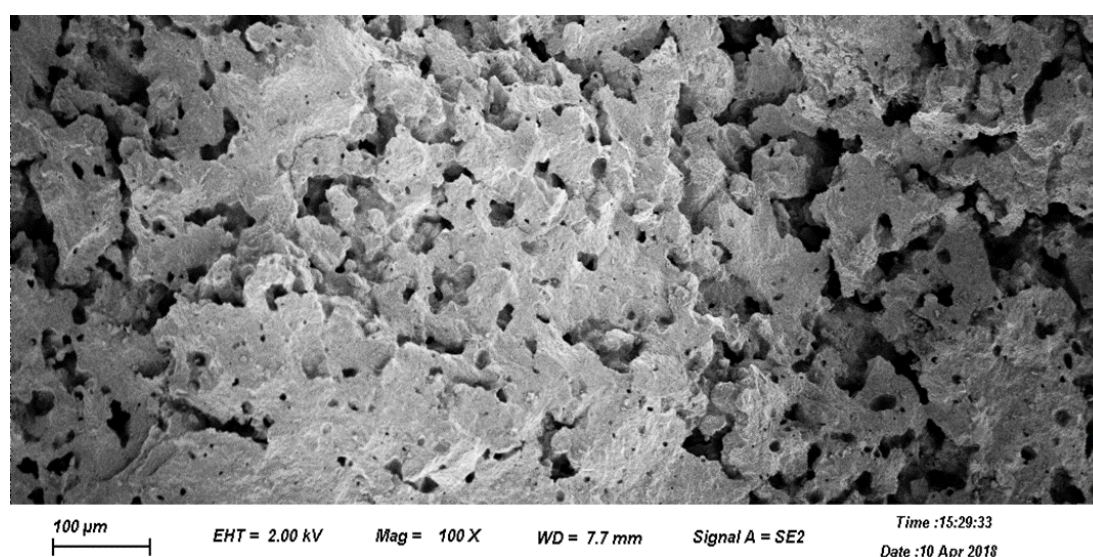


Figure 1. Microstructure of MagA aggregate.

Alumina spinel model castables were formulated according to the recipes and sieve fractions in Table 2. Pre-sintered MA spinel and parts of WFA and TA were replaced with MagA of similar sieve fractions as in the reference castable A-MA-REF. Two different MagA addition levels were chosen. A-MA-18MagA contained 18 wt% MagA, while A-MA-38MagA used 38% MagA. Since this aggregate replacement was based on weight calculation and with the lighter CMA grains compared to the alumina and spinel, the volumetric distribution was not strictly the same, which might explain some differences in vibration flow and flow decay that were measured according to ISO 1927-4:2012, 5.3 using a vibration table as described in ISO 1928-5:2012, 4.3. However, with the introduction of porous MagA aggregates into the castable, an increase of water demand was expected. A-MA-18MagA required 0.4% more water compared to A-MA-REF to achieve a similar initial flow under vibration. The flow dropped in both cases to 25% after 60 min. A-MA-38MagA was cast under vibration with 0.8% more

water than the reference material, but this resulted in an initial flow of only 45% and a fast flow decay. However, the flow was acceptable to shape the samples for the subsequent tests properly.

Table 2. Model castable formulations and granulometry.

Raw Material (wt%)		A-MA-REF	A-MA-18MagA	A-MA-38MagA
White Fused Alumina (WFA)	5–8 mm	15	11	5
Tabular Alumina (TA)	0–6 mm	55	54	40
MagArmour (MagA)	0–10 mm	0	18	38
Magnesium aluminate spinel (MA)	0–1 mm	13	0	0
Reactive alumina	D50 1.5 μ m	11	11	11
Calcium aluminate binder	Secar [®] 71	5	5	5
Polycarboxylate ether-based deflocculant	Refpac [®] 500	1	1	1
Water		+3.6	+4.0	+4.4
Castable sieve analyses (wt%)	5–10 mm	15	15	15
	3–5 mm	20	20	20
	1–3 mm	10	10	10
	0.1–1 mm	19	18	19
	0–0.1 mm	36	37	36

Two samples per formulation and curing condition were cured for 6 h and for 24 h at 20 °C to measure early strength development on prisms of 40 × 40 × 160 mm. Furthermore, two samples per recipe and pre-treatment condition were dried at 110 °C for 24 h and then fired for 3 h at 1100 °C or 3 h at 1550 °C to measure at 20 °C the cold modulus of rupture (CMOR), bulk density (BD), and apparent porosity (AP). The hot modulus of rupture (HMOR) was measured at 1450 °C on two samples that were pre-fired for 30 min at this temperature in the test equipment. The permanent linear change (PLC) of the prisms fired for 3 h at 1100 °C and 1350 °C was measured relative to the sample size achieved after drying at 110 °C. The test results for all these physical properties were expressed as the average of two measurements. The static corrosion tests were conducted with a steel ladle slag in castable cups that were pre-fired at 1600 °C. The slag was kept in the cups during 3 h at 1600 °C. After the experiment, the cups were cut into two parts to allow a macroscopic evaluation of slag penetration and corrosion effects.

Furthermore, a commercial alumina spinel dry-gunning mix (Jinan New E'mei, Jinan, China) was selected as the test material in which about half of the dense alumina aggregates were replaced by the newly designed porous synthetic MagA aggregate. Table 3 summarizes the chemical compositions of these refractory materials. An alumina spinel castable (A-MA-cast) was used in a steel ladle wall and was either repaired by the original alumina spinel dry-gunning mix (A-MA-gun) or by the newly designed MagA-containing alumina spinel dry-gunning mix (MagA-gun).

Table 3. Chemical composition (wt%) of refractory materials for steel ladle trial.

	Al ₂ O ₃	CaO	MgO	SiO ₂
New dry-gunning mix: MagA-gun	78.6	7.5	13.8	0.1
Reference dry-gunning mix: A-MA-gun	87.6	4.5	7.8	0.1
Substrate castable: A-MA-cast	90.7	0.8	7.5	1.0

A repair layer with a thickness of approximately up to 10 cm was sprayed onto the used substrate castable, using either the A-MA-gun or the MagA-gun for the repair. Prior to the repairs, the A-MA-cast surface was cleaned from thick slag layers. Surfaces that showed only thin slag coating or slag penetration into the castable were kept in the wall and served as the substrate for the gunning mix.

At the end of the service life of the MagA-gun repair material, samples for postmortem investigations were taken from the ladle wall and prepared for the detailed microstructure analyses with the scanning electron microscope (SEM) FEI Quant 250 FG (2–5 keV) with elemental analyses by energy dispersive X-ray spectrometry (EDX), Oxford AZtec IE350 SDD Xmax 50 (20 keV). Furthermore, X-ray fluorescence (XRF) was used to determine the chemical compositions (S4 Pioneer Brucker). Measurements were conducted on samples that were prepared by fusion with lithium tetraborate (Perl X3, Panalytical). X-ray diffraction (XRD) was conducted using a Bruker D8 Advance analyzing Cu K radiation at 30 mA and 40 kV for the angles 2θ from 5° to 80° with intervals of 0.0197° .

3. Results and Discussion

3.1. Laboratory Trials with Alumina Spinel Castable Containing Porous MagA Aggregates

As expected, the partially replacement of the dense WFA, TA, and MA spinel aggregates by 18% and 38% of the porous MagA aggregates resulted in a reduced bulk density (Figure 2a) due to the lower grain density of MagA. With 18% MagA, the lightening effect was close to 3%, and with 38% MagA, a density reduction of 8% was achieved. This corresponded directly to material savings of 3% (18% MagA) and 8% (38% MagA) for a given ladle lining configuration. The introduction of the lighter MagA aggregates into the formulations was based on a gravimetric replacement approach for the dense alumina and spinel aggregates as it fit well with the ratio between the different MagA fractions that were generated during the industrial crushing and sieving process.

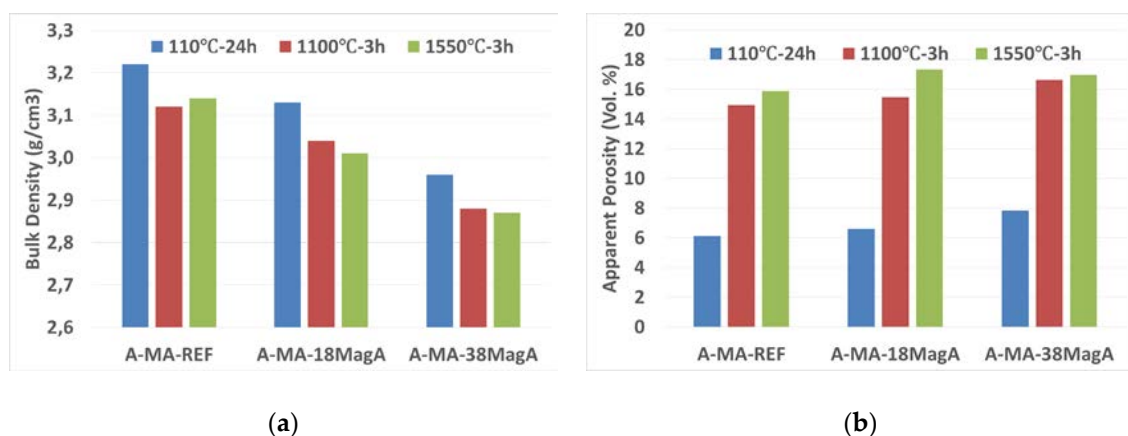


Figure 2. Bulk density (a) and apparent porosity (b) of castables after different heat treatments.

From a volumetric point of view, this created formulations with a slightly higher aggregate volume than in the reference formulation, thus a relatively smaller matrix amount. Since the matrix of a refractory castable contains typically a much higher apparent porosity than the dense high alumina aggregates, an increase of the aggregate volume at the expense of the matrix volume reduced the overall porosity. However, the introduction of MagA into the formulation increased the open porosity in the aggregate part. Overall, the water demand increased, but not as much as one would have expected with a volumetric replacement approach. The increase of the apparent castable porosity was in the range of 1 to 2 vol% (Figure 2b), which is a relatively small increase considering the amount of open pores in the initial MagA grains (approximately 30 vol%). A reason for this moderate increase of open porosity might be that the MagA grains contained hydratable calcium aluminates and that the hydrates might have filled the pores to a certain extent during curing and drying at 110 °C. At high temperatures, the de-hydrated calcium aluminates could further react with available alumina to form CA_2 and CA_6 . These in situ reactions went along with a volume increase, and this additional volume could most likely be accommodated by the pores of MagA.

Despite the slightly higher porosity and lower density, the CMOR (cold modulus of rupture) was not negatively affected (Figure 3a). The strength after 24 h of curing at 20 °C, after drying at 110 °C and firing at 1100 °C, was even slightly increased. The small increase was probably due to the presence of calcium mono-aluminate (CA) in MagA that might partly have dissolved together with the calcium aluminate binder in the mixing water and then contributed to the hydraulic bond. After firing at 1550 °C, the CMOR was reduced. This was in line with the HMOR (hot modulus of rupture) measured at 1450 °C, which also reduced with the addition of MagA (Figure 3b).

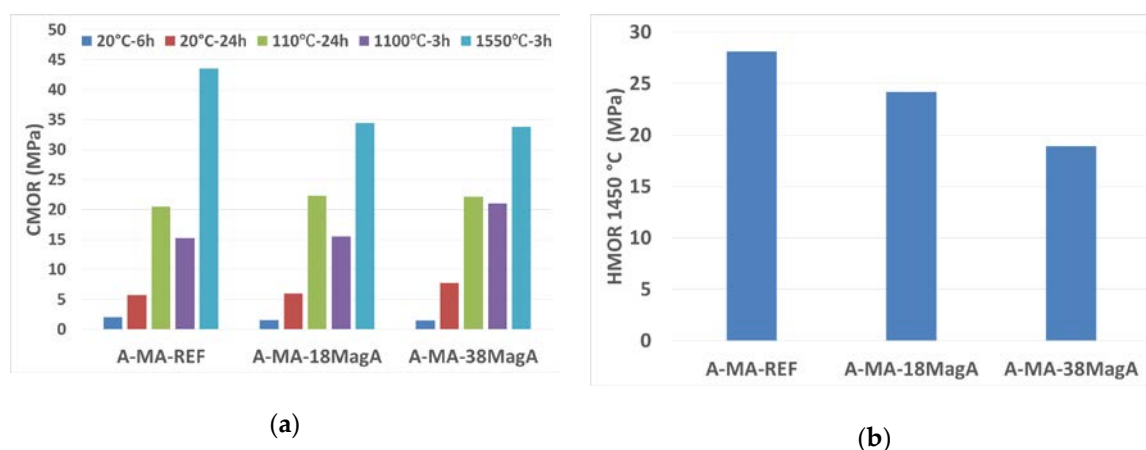


Figure 3. Cold modulus of rupture (CMOR) after curing at 20 °C and after heat treatment (a) and hot modulus of rupture (HMOR) at 1450 °C (b).

The somewhat lower CMOR (1550 °C) and HMOR (1450 °C) might be the consequence of a higher positive PLC (permanent liner change), as shown in Figure 4. This could eventually be explained by a further uptake of alumina into the stoichiometric MA spinel inside the MagA aggregates. Furthermore, the MagA aggregates had the capacity to form some additional CA_6 by reaction of their CA and CA_2 content with alumina, which could also contribute to an expansion. Overall, a slightly higher expansion during the first heat-up of the MagA containing castables might, similarly to the expanding alumina magnesia (AM) castables, have contributed to a reduction of cracks and could result in a densification of the matrix under constraint conditions [15], which could occur in monolithic ladle walls. Similarly to AM castables, this could have a positive effect on the slag penetration resistance of MagA containing castables.

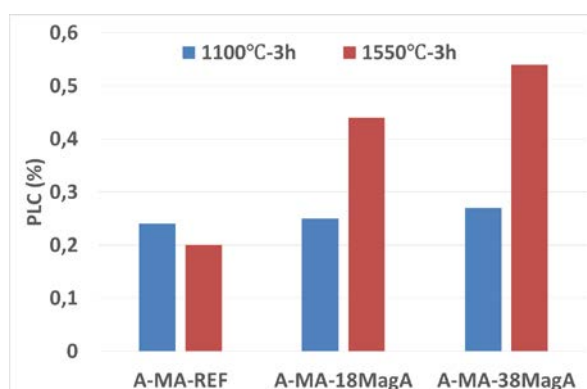


Figure 4. Permanent linear change (PLC) after firing at 1100 °C and 1550 °C.

Furthermore, the increase of total CaO content in the castable with the addition of MagA might have had an impact on the HMOR. The reference castable contained only 1.5% CaO, while it was 3.1% in A-MA-18MagA and 4.9% in A-MA-38MagA. Nevertheless, HMOR remained significantly higher

than for ladle castables based on alumina magnesia that typically need to contain a small amount of silica fume to prevent excessive PLC as a consequence of a high amount of in-situ spinel formation along with CA_6 formation, but also to prevent the hydration of MgO. However, the silica addition affected quite strongly the HMOR of those castables.

Static corrosion trials were performed at 1600 °C for 3 h with cups made from A-MA-REF and A-MA-38MagA castables. They were filled with a Fe_2O_3 -rich and F-containing ladle slag with a C/S ratio of 6.7. The chemical composition is shown in Table 4. Macroscopically, no significant differences could be observed between the two castables (Figure 5). This was remarkable taking into account the significant difference in aggregate porosity and castable density. This was also different from findings with porous alumina aggregates where a stronger penetration was observed [9], but confirmed the studies of Fu et al. [10], who reported an improved performance when using a microporous corundum, and of Chen et al. [6], who found that a porous MA spinel aggregate performed similarly to a dense alumina aggregate.

Table 4. Chemical composition of ladle slag (wt%).

CaO	Al ₂ O ₃	SiO ₂	Fe ₂ O ₃	MgO	TiO ₂	F
2.6	25.8	7.9	5.1	4.4	0.2	1

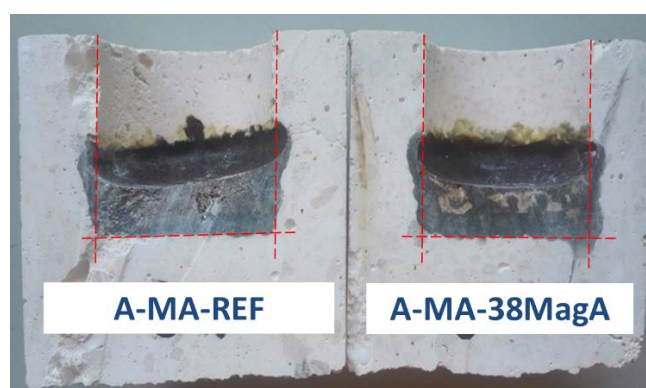


Figure 5. A-MA castables with slag treatment at 1600 °C, 3 h.

3.2. Verification of Laboratory Findings in the Industrial Ladle Trial

In order to verify that the porous MagA could withstand real steel ladle conditions, a trial was conducted using an alumina spinel dry-gunning repair mix as a reference (A-MA-gun) in comparison to a dry-gunning mix (MagA-gun) in which about half of the amount of the dense alumina aggregates was replaced by the porous MagA. Both gunning mixes were applied on a used and cold alumina spinel castable (A-MA-cast). Figure 6 shows the steel ladle in operation with the newly designed MagA-gun in comparison to the original A-MA-gun. The ladle with A-MA-gun had to be taken out of operation 18 heats after the gunning repair due to sever spalling. The first spalling was visible after eight heats. The MagA-gun showed after 21 heats only little spalling and could remain in service for as long as 31 heats.

3.3. Corrosion Mechanism of MagA-Containing Alumina Spinel Dry-Gunning Mix Applied in a Steel Ladle

After 31 heats, samples were taken from the remains of MagA-gun in order to investigate the microstructure along the material profile, from its hot side that was in contact with steel and slag, to the colder interface with the A-MA-cast substrate.

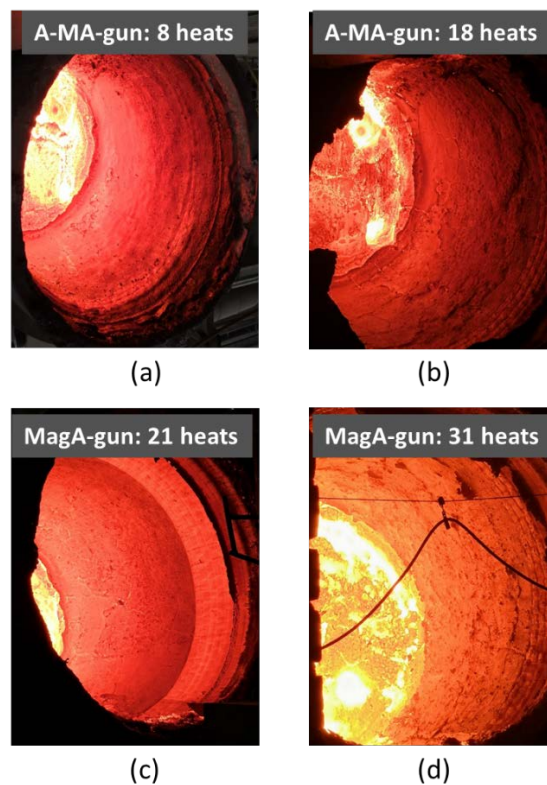


Figure 6. Steel ladles repaired with an A-MA-gun after eight heats in operation (a) and 18 heats (b) versus MagA-gun after 21 (c) and 31 heats (d).

As can be seen in Figure 7, the gunning material had some slag sticking on the hot surface (zone a), showing a slightly darker, probably penetrated zone of approximately 9 mm (zone b), followed by a zone (c–f) with little or no infiltration (9 to 42 mm). Inside that zone, a crack occurred, and it opened up when samples were prepared for microscopy (Fracture Zone e). The backside of the sample, which faced the substrate material, had a thin black layer sticking on it with a thickness of up to 3 mm (Zone g). This thin layer most likely originated from the slag that was still sticking on the substrate castable when the gunning mix was installed in the ladle wall.

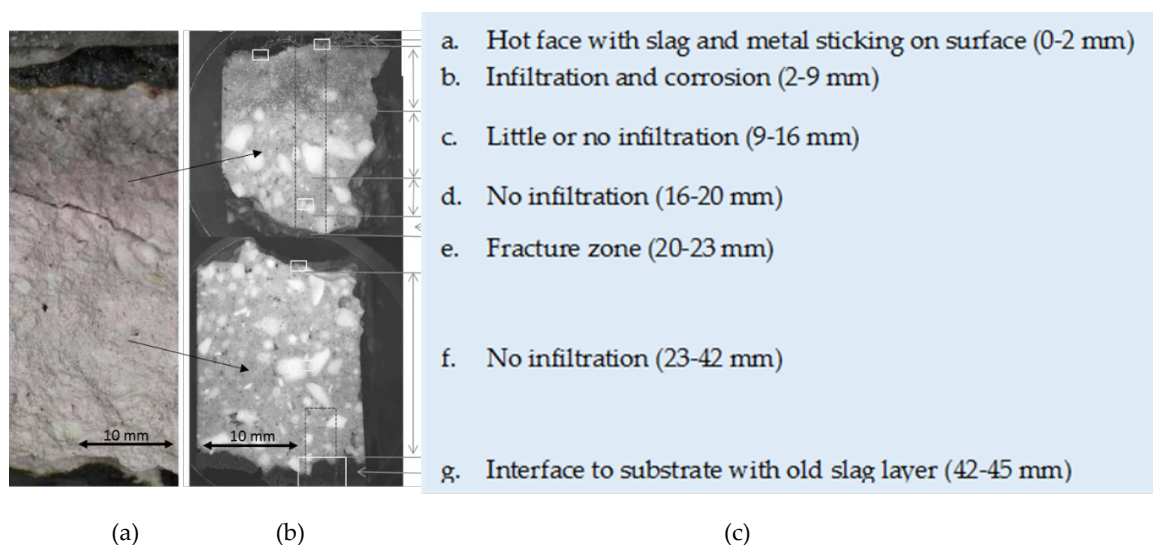


Figure 7. Postmortem sample of MagA-gun after 31 heats before (a) and after cutting (b) and macroscopic observations (c).

To get a better understanding of the underlying mechanisms that led to the improved performance of the MagA-gun during ladle operation, the microstructure was investigated and is described in the following part with the focus on three areas:

- the hot side of the sample, where obviously, some penetration and corrosion took place,
- the center of the sample, which did not show alteration macroscopically, except a macro crack,
- the back side of the gunning mix that was in contact with the castable substrate.

3.3.1. Microstructure at the Hot Face, Zone a (0–2 mm)

A thin metal film stuck to the surface of the sample, separated by a little gap from a layer of iron oxide, mainly FeO and some Fe₂O₃ (Figure 8). Iron oxide did not migrate deeply into the refractory material and remained largely concentrated close to the refractory surface, while manganese was mainly captured by spinel in the first few millimeters of the refractory. That iron oxide layer was up to 250 μm thick and closely connected to the underlying refractory material. In direct contact to the iron oxide, mainly calcium aluminum silicate with a composition close to gehlenite (C₂AS) and manganese-enriched MA spinel grains occurred. A zoom into this zone (a) with the positions of EDX spot analyses is presented in Figure 9a. The analysis indicated that between the gehlenitic areas and the spinel crystals, a probably glassy phase was trapped with a chemical composition including mainly calcium, aluminum, and silicon, but also some manganese, titanium, and fluorine, probably from slag fluxing (Table 5). Furthermore, some areas with an enrichment of hibonite needles (CA₆) were observed (Figure 8), and a zoom into this area (b) is shown in Figure 9b. The EDX analyses also showed here that between the CA₆ needles, mainly phases close to C₂AS composition, spinel, and some other glassy phase were trapped (Table 5). The elemental distribution revealed that iron did not diffuse deeply into the refractory material, while manganese was clearly present up to 400 μm into the repair material, but did not enter the CA₆-enriched area. Although the EDX analyses indicated phases close to C₂AS, the XRD analysis of this front zone did not signal any crystalline C₂AS. Probably glassy calcium aluminum silicate phases with variable compositions were dominating this front zone. The whole front zone showed very little porosity, which obviously prevented slag from deep penetration into the material. As seen with the static corrosion test, despite the presence of the porous MagA grain, no excessive slag penetration was observed. In the case of MagA-containing refractories, the penetration and corrosion front was homogeneous without any preferential penetration through the pores of the MagA grains.

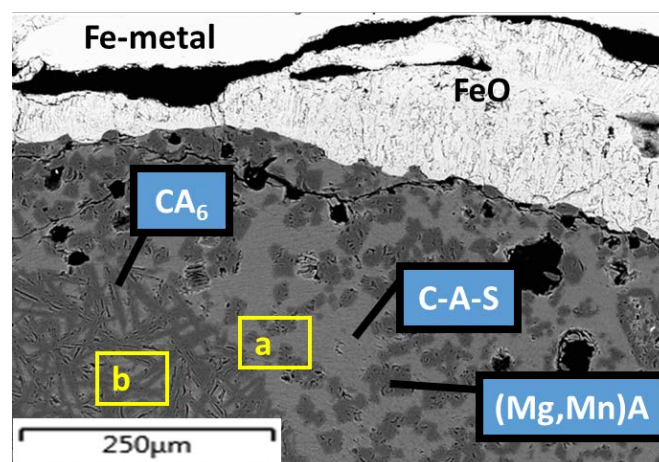


Figure 8. Microstructure of MagA-gun at the hot side.

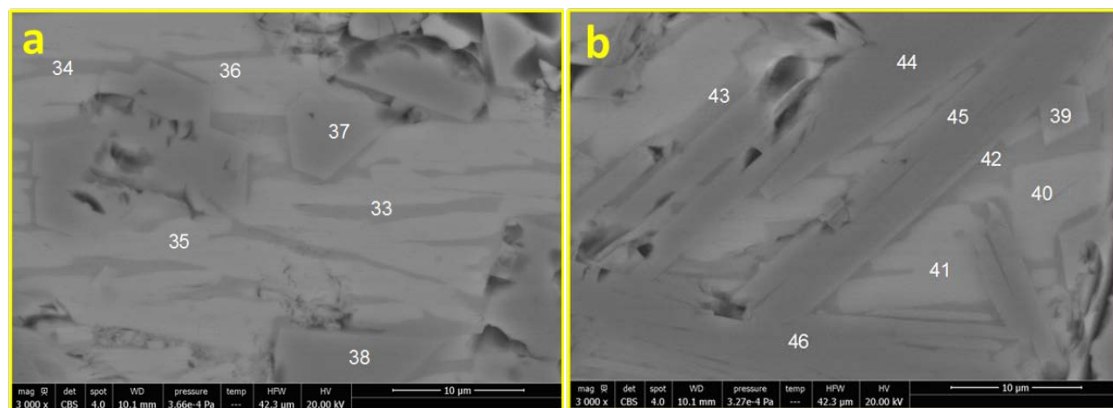


Figure 9. Zoom into Areas a (a) and b (b) of Figure 8 with the positions of EDX-spot analyses.

Table 5. EDX analyses of the points shown in Figure 9a,b.

wt%	Points Indicated in Figure 9a						Points Indicated in Figure 9b							
	33	34	35	36	37	38	39	40	41	42	43	44	45	46
O	42.0	43.1	41.1	41.2	42.8	43.4	42.3	40.4	40.1	42.0	41.8	44.2	44.4	44.1
F	0.6	0.7	nd	nd	nd	nd	nd	nd	nd	1.4	1.1	nd	nd	nd
Na	0.2	0.3	0.1	0.2	nd	nd	nd	0.3	0.2	0.4	0.3	nd	nd	nd
Mg	0.5	0.8	0.2	0.3	6.2	11.8	8.6	0.2	0.4	0.6	0.8	0.4	0.4	0.3
Al	17.6	18.0	18.8	18.8	25.9	37.5	35.2	19.0	19.9	18.4	24.0	48.6	48.5	49.0
Si	14.1	15.9	11.3	11.4	7.9	nd	1.8	11.3	12.0	16.5	14.4	0.5	0.5	0.4
K	0.2	0.3	nd	nd	0.2	nd	nd	nd	nd	0.3	0.2	nd	nd	nd
Ca	22.9	18.2	27.9	27.4	13.0	0.1	2.9	28.3	26.2	17.0	14.0	6.3	6.2	6.2
Ti	0.6	0.8	0.2	0.2	0.5	nd	0.1	nd	0.2	0.7	0.7	nd	nd	nd
Cr	nd	nd	nd	nd	nd	nd	0.3	nd	nd	nd	nd	nd	nd	nd
Mn	1.3	2.1	0.5	0.5	3.3	6.1	7.6	0.5	1.0	2.8	2.6	nd	nd	nd
Fe	nd	nd	nd	nd	0.4	1.1	1.2	nd	nd	nd	nd	nd	nd	nd
Total	100	100	100	100	100	100	100	100	100	100	100	100	100	100
Supposed phase	Glassy phase		C2AS Gehlenite		Glassy phase		(Mg,Mn)Al-Spinel		C2AS Gehlenite		Glassy phase		CA6 Hibonite	

nd = not detected.

To quantify the chemical alteration on the hot side versus the non-penetrated refractory material, samples were taken for XRF measurements from the front side (0–7 mm), from the range 7–13 mm, and 18–35 mm behind the hot face. An increased level of CaO, SiO₂, Fe₂O₃, and Mn₂O₃ at the hot face was confirmed here too (Figure 10), and both Al₂O₃ and MgO were relatively lower than in the original gunning mix. While an increased level of silica and lime was still observed 7–13 mm behind the hot face, both iron oxide and manganese oxide were here almost as low as in the original gunning mix. This low iron- and almost manganese-free silica lime slag penetrated and densified the gunning mix up to approximately 9 mm, as observed with SEM-EDX.

Behind the dense front zone, the refractory material still consisted of MA spinel, CA₆, CA₂, and A as the major refractory phases besides some penetrated calcium silicate that was found with compositions close to gehlenite. Nevertheless, the ratio between A and MA was here significantly lower than in the non-penetrated colder zone. This could mean that the alumina was reacting faster with the penetrating slag than the spinel. However, it has also to be taken into account that in parallel with the reaction with the slag, there was also an in situ reaction between the components of the refractory material that led to the formation of CA₆ from the sintering reaction between alumina and the calcium aluminate phases of the binder and of MagA.

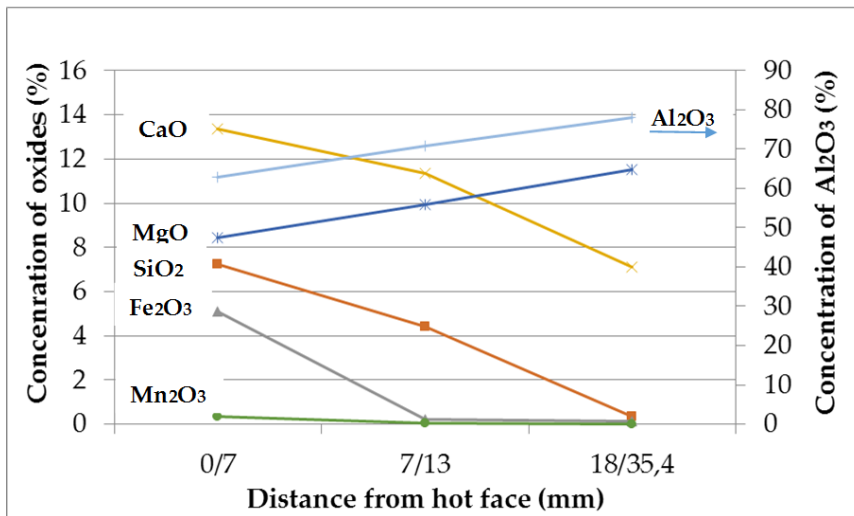


Figure 10. XRF analyses of samples taken at the different distances from the hot side.

3.3.2. Microstructure of the Non-Penetrated Zone f (23–42 mm)

A sample that was taken about 33 mm behind the hot face clearly showed that no penetration had occurred here. Alumina and MagA grains were embedded in a fine-grained matrix (Figure 11a). Neither the pores of the MagA grains, nor the pores in the matrix showed any sign of slag infiltration. EDX analyses (elemental distribution and point analyses) confirmed that the alumina grains reacted with lime from the surrounding calcium aluminate binder or MagA to form a rim consisting of CA₂ (Figure 11b). This might explain why in some cases, the alumina grains seemed to be less well connected to the matrix with some pores at the grain boundaries. This was in contrast to the MagA grains that were well connected with the matrix.

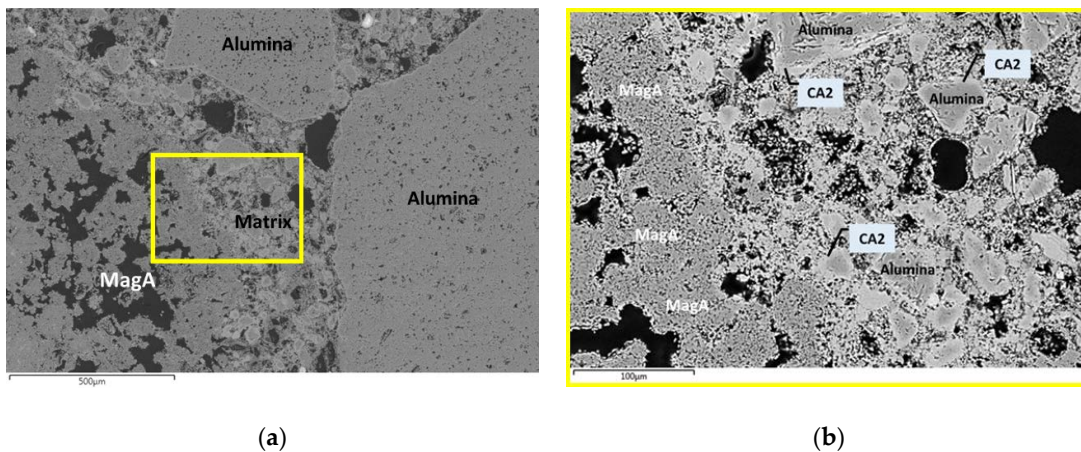


Figure 11. Microstructure of non-penetrated Zone f about 33 mm from hot side (a) and zoom into the indicated matrix area (b).

Since the MagA-gunning mix contained a significant amount of CaO (7.5%), it has a high potential of forming calcium aluminates together with alumina, including the alumina aggregates, as can be seen in Figure 12. A clear rim of calcium aluminate formed around the alumina aggregates.

About 20–42 mm into the material, still some CA was present, either originated from the MagA aggregate or the calcium aluminate binder. This showed that the temperature gradient in the gunning mix was quite high as the temperature was not high enough here to transfer all CA by sintering reaction with alumina into CA₂ or CA₆. Measurements of thermal conductivity will be conducted to quantify the temperature gradient that can be expected in the MagA-containing materials.

The macro crack, which occurred about 20–23 mm behind the hot face, probably opened during cooling of the ladle to ambient temperature, as it was free of any penetration.

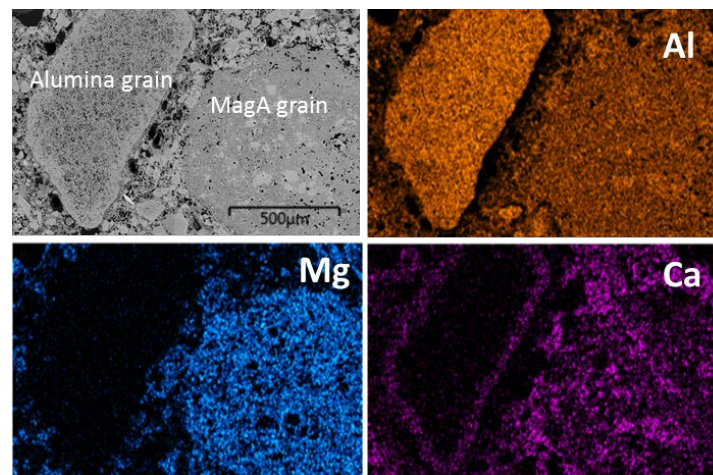


Figure 12. Element distribution in the non-infiltrated zone of the MagA-gun.

3.3.3. Microstructure at the Interface with Substrate, Zone g (42–45 mm)

At the back side of the MagA-gun sample, the contact zone towards the substrate, a thin layer or flakes of iron oxide, present as FeO and Fe₃O₄, were observed. These were most likely the remains of slag that was still sticking on the surface of the substrate when the gunning mix was installed. Into the gunning mix, an iron oxide-enriched thin zone was observed of approximately 500–800 µm. No other elements seemed to have penetrated this specific somewhat iron-enriched zone. XRD and EDX-spot analyses revealed that the iron was mainly present in the form of hercynite (FeAl₂O₄) crystals and occurred predominantly in the calcium aluminate matrix, but in some cases also around or a few microns inside the MagA grains (Figure 13). Interestingly, just next to this iron-enriched thin zone and just a bit closer to the hot side, another thin zone was observed in which calcium and silica were at an elevated level, while iron was not present here. Furthermore, the MagA grains that were present in this Ca-Si-enriched zone showed an increased level of silica only, while neither calcium nor iron was at an elevated level here. With XRD of the sample taken from Zone g (42–45 mm), no silica-containing phases were detected either because the amount was below the detection limit or they were present as glassy phase (Table 6). However, unlike in the non-penetrated Zone f (23–42 mm), CA₂ was the only calcium aluminate phase that was detectable in Zone g. Neither CA nor CA₆, but also no β-alumina were found here.

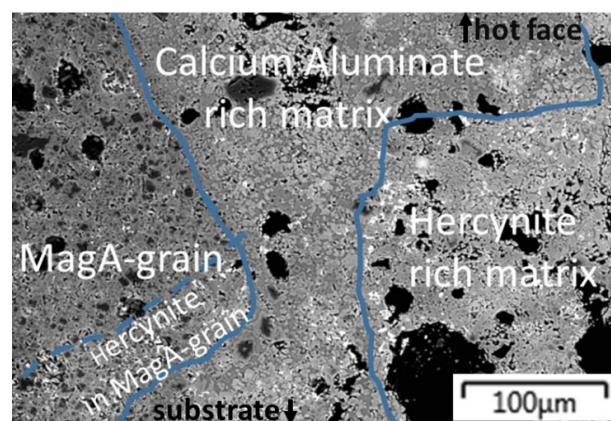


Figure 13. Microstructure close to the interface with the substrate.

Table 6. XRD-phase analyses of the different zones of MagA-gun.

Zone	a	b	c	d	e	f	g
Distance from Hot Face (mm)	0–2	2–9	9–16	16–20	20–23	23–42	42–45
	Hot Face	Infiltration and Corrosion	Less Infiltration and Little Corrosion	Little or No Infiltration and No Visible Corrosion	Fracture Zone	No Infiltration	Inter-Face to Substrate
MA	x	xxx	xxx	xxx	xxx	xxx	xxx
CA	-	-	-	-	x	x	-
CA ₂	-	x	xx	xx	xx	xxx	xx
CA ₆	x	xx	xx	x	x	x	-
α-Al ₂ O ₃	x	x	x	xx	xxx	xxx	xx
β-alumina	-	x	x	xx	x	x	-
C ₂ AS	-	xxx	xxx	x	-	-	-
Fe ₃ O ₄	xxx	-	-	-	-	-	x
FeO	xx	-	-	-	-	-	xx
Fe	xx	-	-	-	-	-	-
FeAl ₂ O ₄	-	-	-	-	-	-	xxx

xxx = high content, xx = medium content, x = low content, - = not detected.

3.4. Complementary Trials with Spinel-Forming Steel Ladle Castable with MagA Addition

To investigate if the porous MagA aggregate could positively influence the thermal cycling resistance of a castable in a steel ladle wall, an industrial trial was conducted in two ladles with a capacity of 120 t of steel. The wall below the slag line of one ladle was cast with a commercial spinel-forming alumina magnesia castable (A-M-cast), while the other ladle used the new recipe (A-M-MagA-cast) that was based on A-M-cast, but with a replacement of 8% dense tabular alumina in the fraction 0–3 mm by 8% porous MagA aggregate of the same granulometry (both castables provided by Jinan New E'mei).

Figure 14a–c shows the ladle wall with A-M-cast after 80, 100, and 144 heats in comparison to A-M-MagA-cast after 55, 109, and 160 heats (Figure 14d–f). The A-M-cast showed significant cracks after 80 heats that further opened during the following heats, as can be seen in Figure 14b, and with layers starting to spall off the wall. After 144 heats, the cracks and spalling became the life-limiting factor, and the ladle had to be taken out of operation without using the full potential of the MgO-C slag line. Contrary to this, the A-M-MagA-cast was significantly less damaged and was still in quite good condition after 160 heats, so that the lifetime of one wall lining was well balanced with the lifetime of three slag zones made of MgO-C.

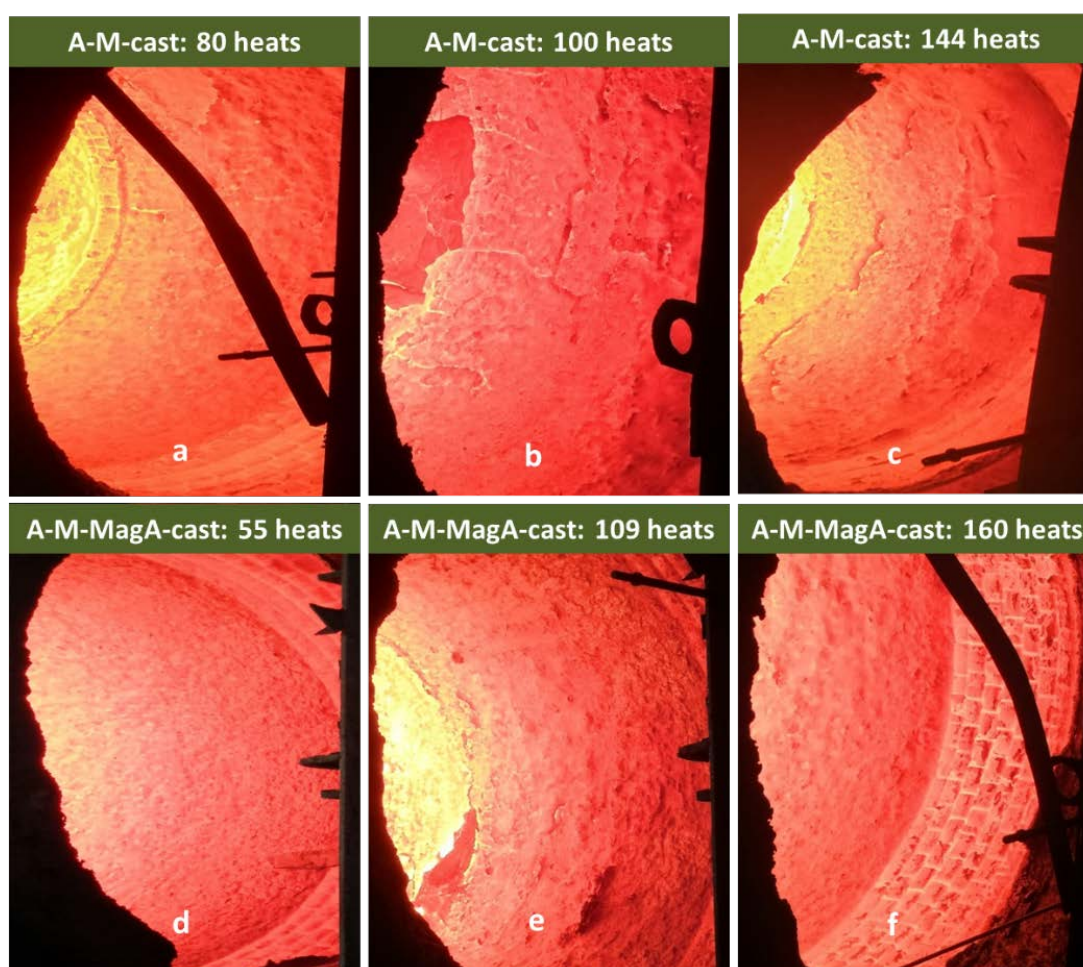


Figure 14. Steel ladle lining with alumina magnesia castable (A-M-cast) after 80 (a), 100 (b), and 144 heats (c) in comparison to the ladle lining with alumina magnesia castable containing 8% MagA (A-M-MagA-cast) after 55 (d), 109 (e), and 160 heats (f).

4. Conclusions and Outlook

The microstructure analyses of the postmortem material from the steel ladle wall showed that slag penetration and subsequent reactions between slag and refractory material created a densified zone with a thickness of up to 1 cm on the hot side of the gunning mix. This dense zone was mainly composed of manganese-enriched spinel crystals and a cluster of CA_6 needles in a matrix of mainly amorphous calcium aluminum silicates, close to a C_2AS composition. This densified zone seemed to block further penetration and to slow down the corrosion. The study showed that the porous MagA aggregates were an interesting alternative to dense alumina and spinel aggregates. Despite their porosity, the penetration and corrosion resistance was not impacted as a dense surface layer was formed that protected the refractory material from deep slag penetration. The MagA-containing gunning mix performed even better than the reference mix that contained only dense alumina and spinel aggregates. The thermomechanical properties altered only very little when replacing dense aggregates by the porous MagA. A slightly higher permanent linear expansion was observed, which could help to minimize crack openings. Indeed, during ladle operation, less crack formation and spalling were observed, both with the MagA-gun and also the A-M-MagA-cast. Overall, the MagA-gun performed significantly longer in the steel ladle than the A-MA-gun. Although the penetration resistance might be a major reason for this improved behavior, also an improved connection to the substrate might have contributed to this positive result. The excellent performance inside a steel ladle when a small amount of MagA was introduced into an alumina magnesia ladle castable supported the hypothesis

that besides sufficient penetration and corrosion resistance, the porous MagA played also a vital role in the improvement of spalling resistance under real ladle operating conditions. Furthermore, this could also be the consequence of an improved thermal cycling resistance, which will be further investigated in the future. The benefits of MagA-containing monolithics are a lower material requirement per ladle lining, an equivalent or even improved service life, and an expected better heat containment, which remains to be confirmed during further investigations in order to evaluate the potential energy savings.

Author Contributions: Conceptualization and writing, C.W. and J.G.; laboratory investigation, M.S. and R.-M.M.; steel ladle trial: J.Z. and J.G.; review and editing, C.P., M.S., J.G., J.Z., and C.W. All authors have read and agree to the published version of the manuscript.

Funding: This research received no external funding.

Conflicts of Interest: The authors declare no conflict of interest.

References

1. Ito, S.; Inuzuka, T. Technical development of refractories for steelmaking processes. *Nippon. Steel Tech. Rep.* **2008**, *98*, 63–70.
2. Braulio, M.; Rigaud, M.; Buhr, A.; Parr, C.; Pandolfelli, V. Spinel-containing alumina-based refractory castables. *Ceram. Int.* **2011**, *37*, 1705–1724. [[CrossRef](#)]
3. Ogata, M. *Development Trend of Refractories in Japan*; ALAFAR Congress: Medellin, Colombia, 2018.
4. Russo, A.A.; Smith, J.D.; O'Malley, R.J.; Richards, V.L. Mechanism for Carbon Transfer from Magnesite-Graphite Ladle Refractories to Ultralow-Carbon Steel. *Iron Steel Technol.* 2016. Available online: https://s3.amazonaws.com/academia.edu.documents/53467294/Mechanism_for_Carbon_Transfer_frof_Magnesite-Graphite_Ladle_Refractories_to_Ultra-Low_Carbon_Steel.pdf?response-content-disposition=inline%3B%20filename%3DMechanism_for_Carbon_Transfer_from_Magne.pdf&X-Amz-Algorithm=AWS4-HMAC-SHA256&X-Amz-Credential=AKIAIWOWYYGZ2Y53UL3A%2F20200318%2Fus-east-1%2Fs3%2Faws4_request&X-Amz-Date=20200318T085613Z&X-Amz-Expires=3600&X-Amz-SignedHeaders=host&X-Amz-Signature=e8cfd1592c9fad78d789b823312a9e732ebc734bd68a438ba219026026dfa0bd (accessed on 18 March 2020).
5. Taira, H.; Nakamura, H. Microwave drying of monolithic refractories. *Nippon. Steel Tech. Rep.* **2008**, *98*, 70–76.
6. Chen, R.R.; He, P.X.; Wang, N.; Mou, J.N.; Gan, F.F. Development of A Low Density Castable for Steel Ladle. Available online: http://www.baosteel.com/english_n/e07technical_n/021301e.pdf (accessed on 26 November 2019).
7. Wöhrmeyer, C.; Parr, C.; Fryda, H.; Auvray, J.-M.; Touzo, B.; Guichard, S. New Spinel Containing Calcium Aluminate Cement for Corrosion Resistant Castables. In Proceedings of the Unified International Technical Conference on Refractories (UNITECR), Kyoto, Japan, August 2011.
8. Auvray, J.-M.; Fryda, H.; Wöhrmeyer, C.; Parr, C.; Pawlig, O.; Martinez, M.M.; Campello, J.R. New insights into corrosion mechanisms of a dense refractory castable containing a novel calcium magnesite alumina binder. In Proceedings of the Int. Colloquium on Refractories, Aachen, Germany, November 2012; pp. 95–98.
9. Yan, W.; Li, N.; Miao, Z.; Liu, G.; Li, Y. Influence of the properties of corundum aggregates on the strength and slag resistance of refractory castables. *J. Ceram. Process. Res.* **2012**, *13*, 278–282.
10. Fu, L.; Gu, H.; Huang, A.; Zhang, M.; Hong, X.; Jin, L. Possible improvements of alumina–magnesite castable by lightweight microporous aggregates. *Ceram. Int.* **2015**, *41*, 1263–1270. [[CrossRef](#)]
11. Nagai, B.; Matsumoto, O.; Isobe, T.; Nishiumi, Y. Wear mechanism of castable for steel ladle by slag. *Taikabutsu Overseas* **1992**, *12*, 15–20.
12. Wöhrmeyer, C.; Parr, C.; Szepizdyn, M.; Zetterström, C.; Touzo, B. Calcium magnesium aluminate aggregates for castables. In Proceedings of the Int. Colloquium on Refractories, Aachen, Germany, 16–17 September 2017.
13. Wöhrmeyer, C.; Szepizdyn, M.; Mineau, R.-M.; Gao, J.; Zhu, Y. How to improve the bonding between used steel ladle castable substrate and dry-gunning repair mix. In Proceedings of the Int Colloquium on Refractories, Aachen, Germany, 25–26 September 2019.

14. Aneziris, C.G.; Gehre, P. Effects of magnesium aluminate spinel raw materials on the material properties of MgO-C refractories. In Proceedings of the Int. Colloquium on Refractories, Aachen, Germany, 28–29 September 2016; pp. 242–245.
15. Braulio, M.A.L.; Morbioli, G.G.; Guilherme, P.; Wöhrmeyer, C.; Szepizdyn, M.; Zetterström, C.; Pandolfelli, V.C.; Parr, C. Constraining Effects on High-Alumina Calcium Magnesium Aluminate-Bonded Castables for Steel Ladles. 2017. Available online: http://unitecr2017.mundodecongresos.com/abstracts/Paper_rbcbhfxcsopirpogsam.pdf (accessed on 18 March 2020).



© 2020 by the authors. Licensee MDPI, Basel, Switzerland. This article is an open access article distributed under the terms and conditions of the Creative Commons Attribution (CC BY) license (<http://creativecommons.org/licenses/by/4.0/>).